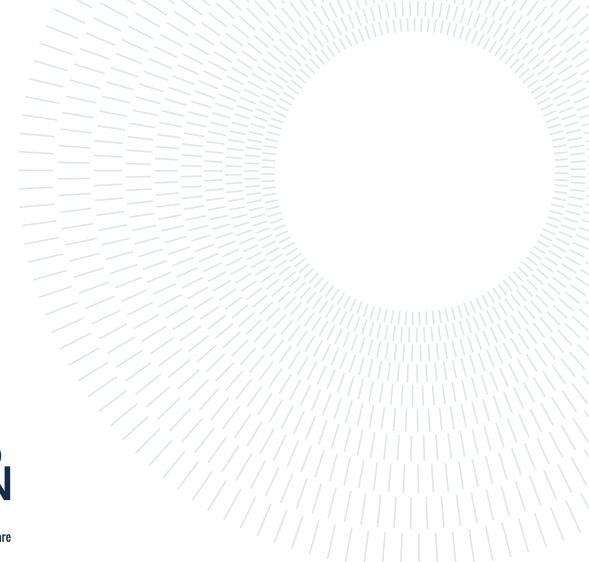




**POLITECNICO
MILANO 1863**

SCUOLA DI INGEGNERIA INDUSTRIALE
E DELL'INFORMAZIONE



EXECUTIVE SUMMARY OF THE THESIS

Preliminary Mechanical Design of a Superconducting Magnet “Canted-Cosine-Theta (CCT)” for a New Gantry for Hadron Therapy

LAUREA MAGISTRALE IN MECHANICAL ENGINEERING - INGEGNERIA MECCANICA

Author: GABRIELE CERUTI

Advisor: MARCO GIGLIO

Co-advisors: LUCIO ROSSI, DIEGO PERINI

Academic year: 2020-2021

1. Introduction and Motivation

Hadron therapy is a medical treatment that uses carbon ions and protons to cure cancer [2]. Carbon ions are really promising for radioresistant tumours, but their use is limited by the size and cost of the needed infrastructure. A relevant element of the infrastructure is the gantry, which significantly improves treatment effectiveness but can weigh hundreds of tons and cost around 25% of the total cost of the facility [1]. This thesis (involved in the collaborations HITRI $plus$ and IFAST [4]) carries out a complete preliminary mechanical design of a new superconducting magnet layout that can help to reduce the gantry’s weight and cost: the Canted-Cosine-Theta (CCT). The CCT design is based on pairs of canted conductor layers (Fig. 1) wound around mandrels (also called formers) nested one inside other (Fig. 2, Fig. 3). Current flows in the two conductors so that the transverse magnetic field components sum and axial field components cancel each other (Fig. 4).

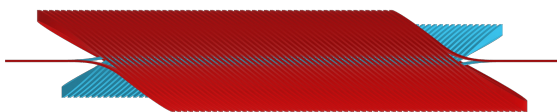


Figure 1: CCT’s inner (blue) and external (red) conductor layers.

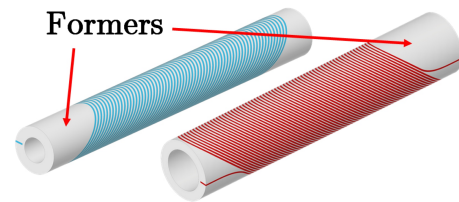


Figure 2: Single CCT layers.

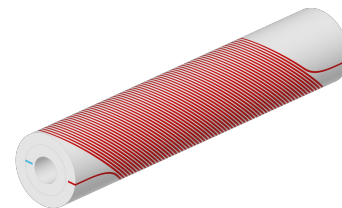


Figure 3: Assembly of single CCT layers.

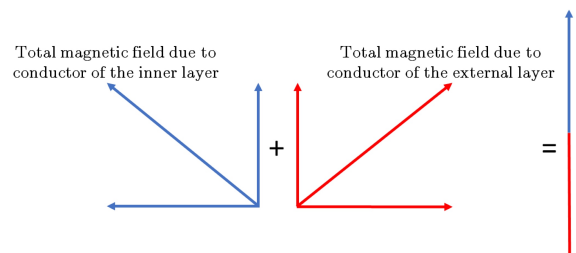


Figure 4: Magnetic field generated by CCT magnet.

The former is a hollow cylinder (or toroid in the case of curved CCT) that contains a groove where the conductor is placed. Moreover, the former is characterized by spar and ribs (Fig. 5) that provide

structural support at the single conductor turn level, reducing the peak of stresses in the conductor up to an order of magnitude with respect to traditional windings [1]. The structural support is fundamental since the coils of the magnet are loaded with Lorentz forces, which tend to deform the magnet and affect the quality of the magnetic field.

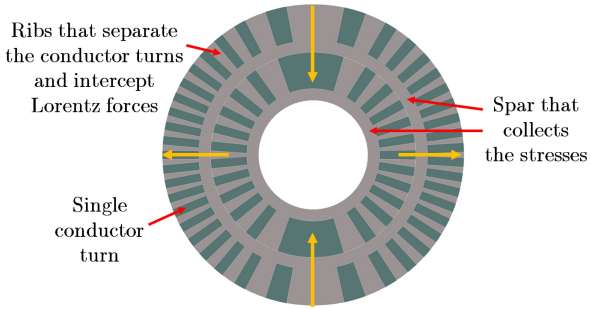


Figure 5: Cross-section of CCT magnet. The orange arrows indicate the resultant of the Lorentz forces.

2. CAD Modelling

The first step of the thesis was generating the geometry of the CCT needed to carry out Finite Element Method (FEM) simulations. Following the procedure shown in [1], it is possible to calculate the equations that describe the central part of the winding path (Fig. 6) for straight and curved CCT. The current leads (the part of the conductor that connects to the power converter, which provides current) and the layer jump (the part of the conductor that connects the inner and external layers) were modelled using cubic Bézier curves (Fig. 6).

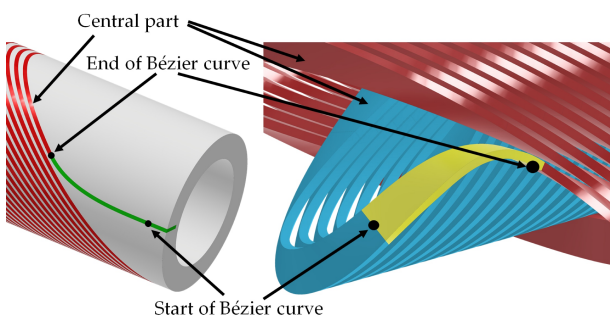


Figure 6: Current lead (green) and layer jump (yellow).

The CAD models (created with Autodesk Inventor – Fig. 7) are completely parametric (controlled by an external Excel sheet), able to update automatically in case of change of parameters' values and can contain up to 8 different magnetic field harmonics [5].

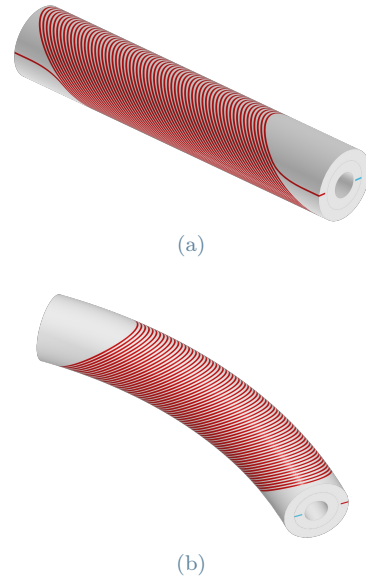


Figure 7: Final CAD models of straight (a) and curved (b) CCT magnet.

3. FEM Simulations

FEM simulations were carried out to evaluate the magnet's behaviour. Each simulation was divided into three steps where the following loads were applied subsequently: external preload by means of screws, cool down from 293 K to 4.2 K (needed to achieve the superconducting state of the conductor in Nb-Ti) and Lorentz force densities (due to energization of the magnet). Simulations started with a first mechanical design (without iron yoke) to represent the most severe case for mechanics. The results showed stresses above the limit. For this reason, a new mechanical design was investigated (Fig. 8).

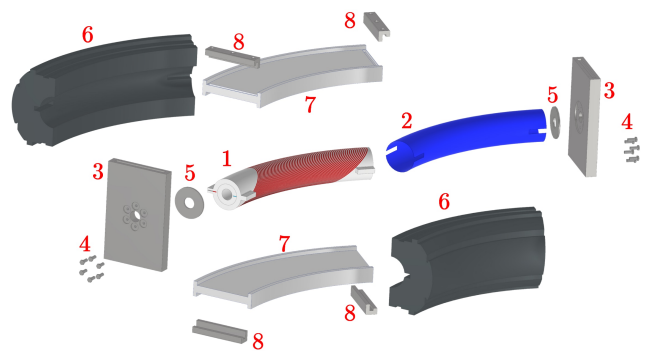


Figure 8: Main components of the mechanical structure surrounding the CCT.

The main components of the new mechanical structure of Fig. 8 are:

1. CCT magnet.
2. Protection material (made of NEMA G10) which insulates and protects the conductor.
3. End plates (made of AISI 316L) which give rigidity to the structure and contain six screws.
4. Screws that contrast Lorentz forces in the mag-

net extremities which tend to make the CCT straight.

5. Small plates (made of AISI 316L) which distribute the action of screws uniformly on the CCT.
6. Iron yoke divided into two halves that must remain attached to the CCT on the magnet midplane to contain the deformations and stresses given by Lorentz forces (Fig. 9). The two halves are separated by a gap whose value was optimized to satisfy two ideal conditions:
 - (a) At the end of the cool down, the gap must be completely closed, while the CCT and iron yoke must have a distance lower than 0.05 mm on the magnet midplane (Fig. 9). This constraint is necessary to maintain a good field quality during the energization of the magnet.
 - (b) When the magnet is energized, CCT and the iron yoke are well in touch on the magnet midplane (Fig. 9) and the gap between the halves of iron yoke must remain closed. This constraint is needed to contrast the Lorentz forces, which ovalize the CCT (Fig. 5) and limit stresses of the CCT.

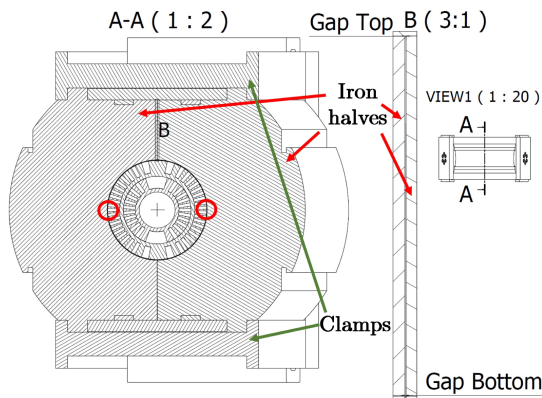


Figure 9: Cross-section of the mechanical structure which surrounds the CCT. Detail B shows the gap between the two parts of iron yoke, which is not constant (at the bottom is smaller than at the top). Red circles indicate the point of contact between CCT and iron yoke on the magnet midplane.

7. Two clamps made of aluminium 6082-T6. All the possible materials for the formers contract more than the iron yoke, leading to detachment between the iron yoke and CCT during cool down. Clamps must avoid this phenomenon, so their material must have thermal contraction higher or equal to one of CCT formers.
8. Four joints with ‘c’ shape (made of AISI 316L) connect the endplates to the rest of the structure.

The structure to suspend the magnet into its cryostat is still under design. For this reason, some

constraints were applied to simulate the simple case where the magnet lays on the ground. The submodelling method (Fig. 10) was used to investigate the stresses with finer mesh. The method consists in doing a first simulation of the whole assembly and a second simulation of the part of interest where displacements from the first simulation are imported as boundary conditions on the cut boundaries. Far from magnet extremities, the geometry of the curved CCT consists of the periodic repetition of a 3D keystone slice (such as the one in Fig. 10c) along the longitudinal direction of the magnet. The loads, stresses and deformations are periodic too, so it is interesting to see the results in the slice at the centre of the CCT. The submodel is wider than a single slice to avoid boundary effects in the slice itself (Fig. 10b).

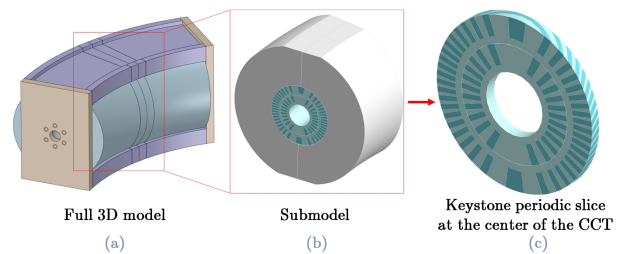


Figure 10: Submodelling applied to the curved CCT.

Two polymers and two metals were investigated for the CCT formers: PEEK GF 30, NEMA G11, aluminium 6082-T6 and aluminium bronze 954. The conductor in Nb-Ti was modelled as a homogenised orthotropic material [3]. The minimum safety factor required for stresses of the formers and the conductor was fixed to 2. This condition was well satisfied in each simulation.

The displacements of the formers were assessed since they change the magnet’s initial shape and define the conductors’ position, affecting the magnetic field and its quality. Cool down makes the CCT smaller but keeps the original magnet’s shape, thus maintaining high field quality. Lorentz forces ovalize the magnet, change its shape, affect the magnetic field and its quality. So, in this preliminary design, it is essential only to evaluate the displacements given by the electromagnetic forces.

The following considerations were done:

- The distribution of displacements is uniform through the 3D periodic slice of the CCT. This permits the evaluation of the results just on the cross-section at the mid of the 3D periodic slice.
- Displacements are calculated with respect to the magnet’s axis (the centre of the cross-section - Fig. 11).
- The radial displacements u_ρ are calculated to check the circularity of the CCT. For this purpose, u_ρ is assessed at different radii (Fig. 11): if the CCT’s cross-section remains circular, the difference of u_ρ for the points which lay on the same radius must remain within a limit. The

circularity of the CCT was evaluated also calculating u_ρ in some significant points and the difference of u_ρ among that points (Fig. 12). The displacements distribution exhibits symmetries that allow considering the significant points in just one quarter of the analyzed cross-section (Fig. 12).

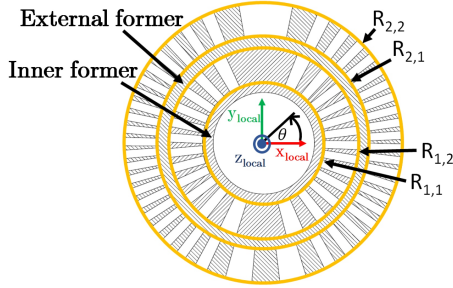


Figure 11: Radii where the difference of radial displacement was evaluated. At the centre, there is the local reference system whose origin coincides with the magnet's axis.

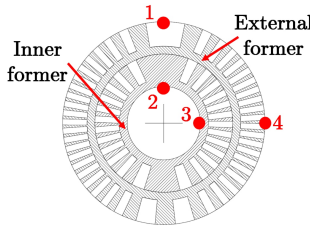


Figure 12: Significant points of the formers to assess the circularity of the CCT. $(u_{\rho,2} - u_{\rho,3})$ must be low, otherwise the CCT is elliptical and not circular. $(u_{\rho,1} - u_{\rho,2})$ and $(u_{\rho,3} - u_{\rho,4})$ must be similar otherwise the thickness of CCT changes too much.

- Azimuthal (circumferential) displacements u_θ are calculated to see if the conductor position changes too much, affecting the magnetic field quality.
- The limit assumed for all the quantities of interest related to the formers' displacements is less than 0.1 mm. This condition was respected in all the simulations for all the quantities.

The same mechanical structure and procedure were applied to straight CCT, obtaining similar results to curved CCT for stresses and formers' displacements.

4. Manufacturing of CCT's Formers

The following considerations can be applied to both straight and curved CCT. In the case of metals, the formers of curved CCT will be produced by milling in the CERN workshop with the following sequence:

1. The initial tube (already bent) is longitudinally split into two parts by a saw or a milling tool. This permits much easier machining of the inner

part of the tube. The machining of the tube's inner area is needed to achieve the geometrical tolerances required to nest the two formers and insert the vacuum chamber hosting the particle beam.

2. Roughing and finishing by milling of the tube's inner area (Fig. 13):

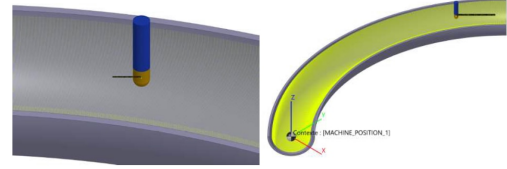


Figure 13: One half of the curved tube with the milling tool (blue). The yellow colour indicates the machined area (Courtesy of Karol Sciborn).

3. Brazing of the two halves of the single tubes.
4. Manufacture of the supports necessary to block the tube during the groove machining (Fig. 14).
5. External diameter roughing and finishing.
6. Milling (roughing and finishing) of the external part of the tube to generate the groove and the final former (Fig. 14).

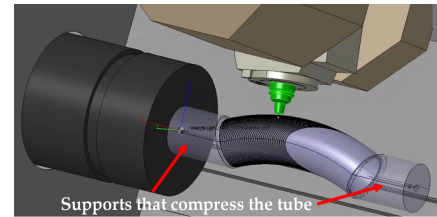


Figure 14: Machining of the former's groove where the conductor is inserted (Courtesy of Karol Sciborn).

In the case of PEEK GF 30 (the main candidate formers' material), the sequence changes due to the availability of raw material that can be found in plates only:

1. The process starts with plates, which will be assembled to make the whole former. Each plate is machined to create the aperture of the former and give the external shape needed for the next step (Fig. 15):

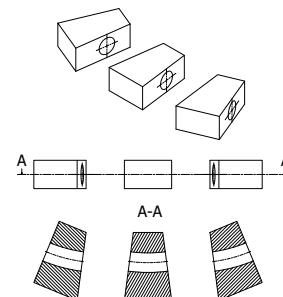


Figure 15: Starting plates after the machining.

2. The single plates are glued (Fig. 16):

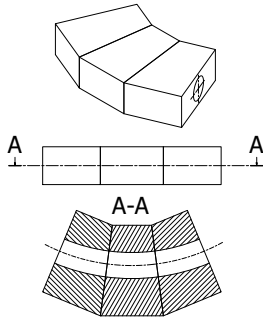


Figure 16: Plates glued.

3. The glued plates are machined to generate the groove and the final shape of the former (Fig. 17). The generation of the groove must be done after gluing the single plates to avoid discontinuities among the grooves, which can cause breakdowns.

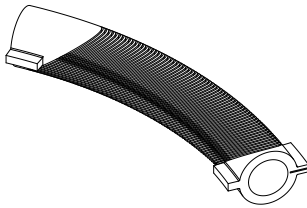


Figure 17: Final former.

Additive manufacturing was considered, but, for the time being, the cost is decidedly higher than machining. Moreover, the achievable mechanical tolerances and roughness are much worse than the limits required by this application.

5. Assembly Process

The assembly procedure uses tools relatively simple and does not need heavy presses or complex curved elements. This is a significant advantage with respect to the traditional design, which requires large presses of about 600-800 tonnes per meter of magnet length. The main steps of the assembly process are:

1. Assembly starts on marble on a horizontal plane where the keystone laminations (Fig. 18) of one iron yoke half are placed vertically. Mechanical stoppers keep laminations in the correct position (Fig. 19).



Figure 18: Single lamination of one iron yoke half.

2. When all the laminations are placed, some keys are added and spot-welded to the laminations (Fig. 19) to make a single iron yoke half.

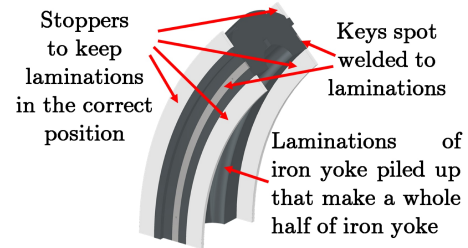


Figure 19: Single laminations of iron yoke piled up, keys and mechanical stoppers.

3. Stoppers are removed, and the half of the iron yoke is placed horizontally on the plane. Some tools (just schematized in Fig. 20) will be used to clamp the half of iron yoke to the ground and leave access to the lower part of the structure to insert the clamps and new mechanical stoppers (Fig. 21).

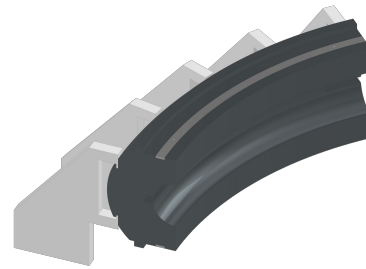


Figure 20: First iron yoke half placed horizontally and clamped to the ground by some tools.

4. The CCT is inserted and attached to iron yoke with a temporary support on both extremities of the magnet. Two mechanical stoppers are fixed to the half of the iron yoke. These stoppers are needed to place the other half of iron yoke in the correct position keeping the gap between the two halves opened (Fig. 21). The stoppers must have high thermal contraction to not interfere with the rest of the structure during the operational phase.

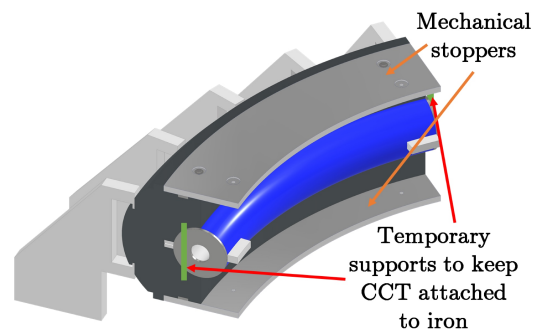


Figure 21: Magnet is kept attached to iron yoke with two temporary supports (green area). Addition of new mechanical stoppers to the structure.

- The steps from 1 to 3 are repeated for the other half of the iron yoke which is pushed against the mechanical stoppers. After this operation, the temporary supports which keep the CCT attached to iron yoke are removed. Then the aluminium clamps are heated and placed in their position to shrink fit with iron yoke (Fig. 22).

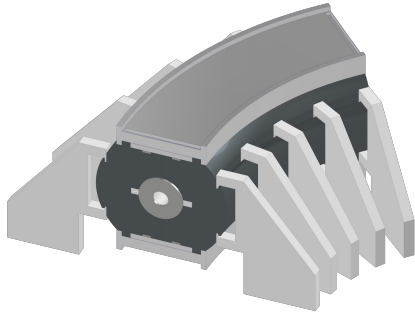


Figure 22: The tools that sustain the two halves of the iron yoke slide horizontally and push one half towards the other until there is contact with the mechanical stoppers. After this procedure, the temporary supports of CCT are removed and the two aluminium clamps are added.

- When aluminium clamps cool down, the end plates, ‘c’ shape joints and screws are added to obtain the final structure (Fig. 23).

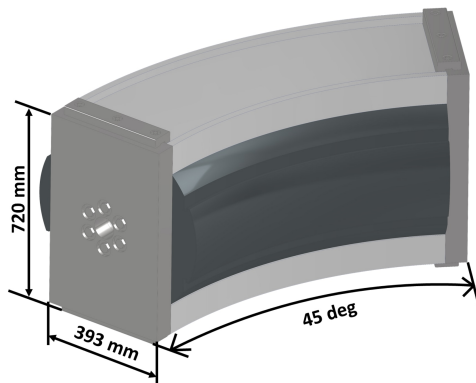


Figure 23: Final mechanical structure surrounding the CCT magnet.

6. Conclusions and Future Developments

The thesis performed a complete preliminary mechanical design of curved and straight CCT magnets. The results of this study are:

- The equations and methods that permit the magnet’s geometry generation by CAD software. Specifically, the generated CAD model is fully parametric, able to update automatically and can represent many magnetic field harmonics [5] combinations.
- A mechanical design was studied for curved and straight CCT to keep stresses and displacements

below the specified limits. The simulations carried out demonstrated that the goal was achieved.

- Development of the methods needed to machine and assembly the magnets.

Now, the project will continue with the following tasks:

- Machining, impregnation and winding tests.
- Mechanical simulations of the curved CCT with the new parameters required by the HITRIplus collaboration and more detailed geometry of the conductor.
- Definition of the construction drawings for the final demonstrators.
- Assembly of the magnet demonstrators around March 2024 for HITRIplus, June 2024 (Nb-Ti conductor) and October 2024 (conductor in HTS - High Temperature Superconductor) for IFAST.

7. Acknowledgements

From the bottom of my heart, I would like to thank all my amazing supervisors from CERN – MME, INFN – LASA and Politecnico di Milano whose support was fundamental. I will never thank them enough: Lucio Rossi, Diego Perini, Marco Giglio, Ernesto De Matteis, Samuele Mariotto, Stefano Sorti, Marco Masci, Jorge Guardia Valenzuela and Federico Carra. Moreover, I would like to thank Prof. Carlo Colombini, who has a lot of merit for making me interested in scientific research. I am very grateful also to God for protecting me over all these years.

References

- Lucas Nathan Brouwer. *Canted-cosine-theta superconducting accelerator magnets for high energy physics and ion beam cancer therapy*. University of California, Berkeley, 2015.
- Alberto Degiovanni and Ugo Amaldi. History of hadron therapy accelerators. *Physica medica*, 31(4):322–332, 2015.
- R Ortwein, J Blocki, P Wachal, G Kirby, and J van Nugteren. Fem modeling of multilayer canted cosine theta (cct) magnets with orthotropic material properties. *Cryogenics*, 107:103041, 2020.
- Lucio Rossi, Gabriele Ceruti, Diego Perini, et al. A european collaboration to investigate superconducting magnets for next generation heavy ion therapy. *IEEE Transactions on Applied Superconductivity*, 32(4):1–7, 2022.
- Ezio Todesco. Magnetic design of superconducting magnets. *arXiv preprint arXiv:1501.07149*, 2015.